PSD-95 and SAP97 Exhibit Distinct Mechanisms for Regulating K^+ Channel Surface Expression and Clustering

Amanda M. Tiffany,*‡ Louis N. Manganas,*‡§ Eunjoon Kim,§ Yi-Ping Hsueh,§ Morgan Sheng,§ and James S. Trimmer*‡§

*Department of Biochemistry and Cell Biology, ‡Institute for Cell and Developmental Biology, State University of New York, Stony Brook, New York 11794-5215; and §Howard Hughes Medical Institute, Massachusetts General Hospital, Department of Neurobiology, Harvard Medical School, Boston, Massachusetts 02214

Abstract. Mechanisms of ion channel clustering by cytoplasmic membrane-associated guanylate kinases such as postsynaptic density 95 (PSD-95) and synapse-associated protein 97 (SAP97) are poorly understood. Here, we investigated the interaction of PSD-95 and SAP97 with voltage-gated or Kv K^+ channels. Using Kv channels with different surface expression properties, we found that clustering by PSD-95 depended on channel cell surface expression. Moreover, PSD-95–induced clusters of Kv1 K^+ channels were present on the cell surface. This was most dramatically demonstrated for Kv1.2 K^+ channels, where surface expression and clustering by PSD-95 were coincidentally promoted by coexpression with cytoplasmic Kvβ subunits. Consistent with a mechanism of plasma membrane channel–PSD-95 binding, coexpression with PSD-95 did not affect the intrinsic surface expression characteristics of the different Kv channels. In contrast, the interaction of Kv1 channels with SAP97 was independent of Kv1 surface expression, occurred intracellularly, and prevented further biosynthetic trafficking of Kv1 channels. As such, SAP97 binding caused an intracellular accumulation of each Kv1 channel tested, through the accretion of SAP97 channel clusters in large (3–5 μm) ER-derived intracellular membrane vesicles. Together, these data show that ion channel clustering by PSD-95 and SAP97 occurs by distinct mechanisms, and suggests that these channel-clustering proteins may play diverse roles in regulating the abundance and distribution of channels at synapses and other neuronal membrane specializations.

Key words: ion channel localization • protein binding • COS cells • membrane proteins • nerve tissue proteins

Introduction

The efficient reception, processing, and transmission of information in neurons is dependent on the precise subcellular distribution of ion channels and receptors in discrete plasma membrane domains (Sheng and Wyszynski, 1997). Three distinct sets of biosynthetic events are thought to be responsible for determining the ultimate distribution of these channels. The first, which occurs in the ER, consists of subunit assembly, folding, and export. The second set of events are associated with the subsequent targeting of the channel polypeptide to its proper subcellular location. This requires sorting machinery present in the TGN. Finally, the retention of the channel occurs at its appropriate plasma membrane locale through direct or indirect interaction with the cytoskeleton. Even though the fundamental molecular processes regulating ion channel expression have been the subject of intense investigation, the details of posttranslational events responsible for regulating the abundance and distribution of channels are only beginning to be defined (Trimmer, 1999).

Voltage-sensitive or Kv K^+ channels are crucial and diverse elements that regulate electrical activity in excitable cells. Kv channels consist of four pore-forming and voltage-sensing polytopic transmembrane α subunits, usually associated with up to four cytoplasmic β subunits (Trimmer, 1998b). Over a dozen Kv channel α subunit genes are expressed in the mammalian nervous system (Chandy and Gutman, 1995) and, within neurons distinct, Kv channels exhibit strikingly different localizations (Trimmer and Rhodes, 1999). For example, certain members (Kv1.1 and Kv1.2) of the *Shaker*-related or voltage-gated K^+channel subfamily 1 member(Kv1)[1] of Kv channels are found precisely localized in juxtaparanodal regions of myelinated

Address correspondence to Dr. James S. Trimmer, Department of Biochemistry and Cell Biology, SUNY at Stony Brook, Stony Brook, NY 11794-5215. Tel.: (516) 632-9171. Fax: (516) 632-9714. E-mail: james.trimmer@sunysb.edu

[1]*Abbreviations used in this paper:* GST, glutathione-S-transferase; Kv1, voltage-gated K^+ channel subfamily 1 member; LCA, *Lens culinaris* lectin; MAGUK, membrane-associated guanylate kinase; PSD-95, postsynaptic density 95; SAP97, synapse-associated protein 97.

axons in both the central (Wang et al., 1993; Rhodes et al., 1997) and peripheral nervous systems (Rasband et al., 1998), and in terminal fields associated with unmyelinated central nervous system axons (Trimmer and Rhodes, 1999). In contrast, Kv1.4 is found in dense patches on presynaptic swellings adjacent to nerve terminals, and on the axon shafts of certain neurons (Cooper et al., 1998). Other Kv channels are found in similarly restricted, but distinct, localizations (Trimmer and Rhodes, 1999). While some insights into the domains responsible for Kv channel localization have been obtained (Scannevin et al., 1996), the precise cellular mechanisms that exist to generate and maintain the wide array of restricted distributions of Kv channels observed in the mammalian brain remain to be elucidated (Scannevin and Trimmer, 1997).

Membrane-associated guanylate kinases (MAGUKs) are attractive candidates as important determinants of localization of a wide array of neuronal proteins, including Kv channels (Sheng and Wyszynski, 1997). Postsynaptic density 95 (PSD-95), the prototypic member of this family, was found to bind to the COOH-terminal cytoplasmic residues of Kv1 α subunits in a yeast two-hybrid screen (Kim et al., 1995). PSD-95 colocalizes with the Kv1.2 α subunit in cerebellar basket cell presynaptic terminals (Kim et al., 1995; Laube et al., 1996). Mutational (Kim et al., 1995) and structural (Doyle et al., 1996) analyses revealed that PSD-95 and other MAGUKs, such as synapse-associated protein 97 (SAP97) and chapsyn-110, bind to a consensus PSD-95/DIg/ZO-1 (PDZ)-binding sequence (xS/TxV) at the COOH terminus of Kv1 channels via either of the first two of the three PDZ domains located near the PSD-95 NH_2 terminus. Coexpression of MAGUKs and Kv1 α subunits in transfected cells leads to the reciprocal coclustering of the respective proteins (Kim et al., 1995; Kim and Sheng, 1996). However, despite the presence of a consensus PDZ-binding sequence (xS/TxV) at their COOH termini (Chandy and Gutman, 1995), different Kv1 α subunits exhibit strikingly different clustering efficiencies when coexpressed with PSD-95 (Kim and Sheng, 1996). In addition to clustering channels, PSD-95 has also been shown to upregulate the cell surface expression of at least one ion channel (Horio et al., 1997). Whereas cytoplasmic Kvβ subunits are known to increase the surface expression of Kv1 channels (Shi et al., 1996; Accili et al., 1997, 1998), the effect of MAGUKs on Kv1 channel surface expression have not been investigated.

In this study, we show that the interaction of Kv1 channels with MAGUKs varies widely among members of the two protein families. By systematically characterizing the association of different Kv1 K^+ channels with PSD-95 and SAP97, we find evidence for distinct differences in the mechanisms whereby channel–MAGUK interaction occurs. These differences lead to differential effects on both channel clustering and surface expression, suggesting that MAGUKs may play important and diverse roles in the regulating both the abundance and distribution of ion channels.

Materials and Methods

Materials

All materials not specifically identified were purchased from Sigma Chemical Co. or Boehringer Mannheim.

Antibodies

Rabbit polyclonal (Kv1.1C, Kv1.2C, and Kv1.4N) and mouse monoclonal (anti-Kv1.4: K13/31) antibodies against the cytoplasmic domains of K^+ channel α-subunits used in these studies have been described previously (Rhodes et al., 1995; Bekele-Arcuri et al., 1996; Rhodes et al., 1996; Shi et al., 1996). Antibodies against ectodomains of K^+ channel α subunits were raised against synthetic peptides or fusion proteins corresponding to sequences in the S1-S2 extracellular loop (see Shih and Goldin, 1997, for determination of K^+ channel topology). The following sequences were used, synthetic peptides: Kv1.1, ELKDDKDFTGTIHRIDNTC (amino acids 191–208); Kv1.2, CNEDMHGGGVTFHTYSNSTIGY (amino acids 192–212); and glutathione-S-transferase (GST) fusion protein, Kv1.4 (amino acids 336–370). The anti-Kv1.2 and anti-Kv1.4 external antibodies were made as polyclonal antibodies in rabbits. The anti-Kv1.1 external antibody was a mouse mAb K36/15 (IgG_{2a}). The monoclonal anti–PSD-95 antibody K28/86 (IgG_1) was raised against a GST fusion protein, GST-KAP1.13, containing amino acids 77–299 of human PSD-95 (clone 2; Kim et al., 1995). Immunizations of mice and the production of hybridoma cell lines were performed essentially as described (Bekele-Arcuri et al., 1996). Screening of hybridoma culture supernatants by ELISA assay against the peptide or fusion protein immunogen, indirect immunofluorescence on transfected COS-1 cells, and immunoblotting of rat brain membranes were performed as described (Bekele-Arcuri et al., 1996). Hybridomas were grown in Balb/c mice for production of ascites fluid. K36/15 and K28/86 immunoglobulins were purified by ammonium sulfate precipitation followed by DEAE chromatography, as described in Trimmer et al. (1985).

Transient Transfection of COS-1 Cells

Cells were transfected with mammalian expression vectors for various K^+ channel α- and β-subunit polypeptides (Nakahira et al., 1996) and for PSD-95 and SAP97 (Kim et al., 1995; Kim and Sheng, 1996) by the calcium phosphate precipitation method (Trimmer, 1998a). Cells were seeded at 10% confluence (for biochemical analysis) or 1% confluence (for immunofluorescence) and grown at 37°C in DME containing 10% calf serum. The calcium phosphate DNA mixture was added within 24 h of seeding, when cells were approximately twice the original plating density, and left for 18–24 h. The transfection media was removed and, after the addition of fresh media, the cells were incubated at 37°C for an additional 24 h.

Immunofluorescence Staining of Transfected COS-1 Cells

Cells expressing various combinations of K^+ channel α- and β-subunit polypeptides, PSD-95 and SAP97, were stained 48 h after transfection. Two different staining protocols were employed. The first is a modification of the surface immunofluorescence protocol (Shi et al., 1996). Cells were washed three times in PBS (10 mM phosphate buffer, pH 7.4, and 0.15 M NaCl) containing 1 mM $MgCl_2$ and 1 mM $CaCl_2$, and then fixed in the same buffer containing 4% paraformaldehyde for 30 min at 4°C. After three washes with PBS, nonspecific protein binding sites were blocked with BLOTTO (4% nonfat dry milk powder in TBS [10 mM Tris-HCl, pH 7.5, and 0.15 M NaCl] for 1 h at room temperature, and then incubated with affinity-purified rabbit polyclonal or mouse monoclonal ectodomain–directed antibodies for 1 h at room temperature. After washing three times with BLOTTO, cells were permeabilized with BLOTTO containing 0.1% Triton X-100 (BLOTTO + T) for 1 h at room temperature. This was followed by incubation with mouse monoclonal cytoplasmically directed antibodies for 1 h at room temperature. Cells were washed three times in BLOTTO + T, incubated with Texas red goat anti–rabbit and FITC goat anti–mouse (for Kv1.2 and Kv1.4) or, for Kv1.1, Texas red goat anti–mouse IgG_{2a} (for external K36/15) and FITC goat anti–mouse IgG_1 (for cytoplasmic K20/78; Bekele-Arcuri et al., 1996) diluted in BLOTTO + T for 1 h, and washed three times with PBS containing 0.1% Triton X-100.

The second staining method used a permeabilization with 0.1% Triton X-100 during fixation. This allowed full access to the total (surface and intracellular) pools of channel subunits and MAGUKs. Cells were viewed under indirect immunofluorescence on a Zeiss Axioskop microscope, and scored for fluorescence on narrow wavelength fluorescein and Texas red filter sets. Three independent dishes were scored for each treatment. Values represent the mean ± SD of values determined from 50 transfected cells from each dish.

Confocal Microscopy

Confocal images were generated on a Zeiss LSM510 laser scanning confocal microscope system with an Axiovert microscope using a 63× plan neofluar NA 1.25 objective. Texas red (red) immunofluorescence signals were obtained using a 560-nm-long pass filter after excitation with a helium neon laser at 543 nm. FITC (green) immunofluorescence signals were obtained using a 505–530-band pass filter after excitation with an Argon laser at 488 nm. Red and green signals were generated and collected individually on a frame-by-frame basis. Similar pinhole sizes and amplifier settings were used to obtain all images, and no further manipulation of image files was performed. Each individual image represents a three-dimensional projection of the entire cell derived from a z-series taken as an average of eight sweeps at 1,024 × 1,024 resolution, and viewed en face relative to the apical surface. Projections were exported as Photoshop files for presentation.

SDS-PAGE and Immunoblots

To harvest cells and prepare detergent lysates, COS-1 cells were washed twice in ice-cold PBS, and then lysed in the dish for 5 min on ice in an ice-cold lysis buffer solution (TBS, pH 8.0, 5 mM EDTA, 1% Triton X-100, 1 mM iodoacetamide, and a protease inhibitor cocktail [2 μg/ml aprotinin, 1 μg/ml leupeptin, 2 μg/ml antipain, 10 μg/ml benzamidine, and 0.2 mM PMSF]). Cell lysates were harvested with a cell scraper and incubated for an additional 5 min on ice. The crude lysate was spun in a refrigerated microcentrifuge for 5 min at 14,000 *g* to pellet nuclei and debris, and the resulting supernatant was saved for analysis.

For immunoblots, the cleared lysate was added to an equal volume of 2× reducing SDS sample buffer, boiled, and fractionated on 9% polyacrylamide–SDS gels (Shi et al., 1994). Lauryl sulfate (Sigma Chemical Co.) was the SDS source used for all SDS-PAGE to accentuate relative molecular mass differences between different forms of Kv1 α subunits (Shi et al., 1994). After electrophoretic transfer to nitrocellulose paper, the resulting blots were blocked in BLOTTO, incubated for 1 h in Blotto containing purified mouse monoclonal K13/31 IgG at 10 mg/ml. Blots were washed three times in Blotto for 30 min total, incubated in HRP-conjugated secondary antibody (1:2,000 dilution in Blotto) for 1 h, and washed in PBS three times for 30 min total. The blots were incubated in substrate for enhanced chemiluminescence for 1 min and autoradiographed on preflashed (to $OD_{545} = 0.15$) Fuji RX film.

Results

Highly Related K^+ Channel α-Subunits Have Dramatically Different Cell Surface Expression Efficiencies

Members of the mammalian *Shaker* (Kv1) family of K^+ channel α subunits exhibit a high degree of overall relatedness (60–80% identity at the amino acid level; Chandy and Gutman, 1995). However, when expressed as homotetramers in transfected mammalian cell lines, the subcellular staining patterns of the expressed channels dramatically differ (Bekele-Arcuri et al., 1996). To address if these differences in staining pattern represented differences in cell surface expression, we employed a double staining procedure, similar to that used by us previously in studies of Kv1.2 (Shi et al., 1996). We generated rabbit polyclonal or mouse mAbs to distinct externally and internally directed sites on each Kv1 channel. Intact (i.e., unpermeabilized) cells were stained first with the appropriate rabbit polyclonal ectodomain–directed antibody to assay for channel surface expression, followed by permeabilization and staining with the cytoplasmically directed mouse mAb to visualize the total cellular pool of channel subunits.

Virtually all cells expressing Kv1.1 exhibited an identical intracellular staining pattern (Fig. 1 A). This staining pattern is indicative of ER retention and correlated with a lack of staining of intact (i.e., unpermeabilized) cells with an antibody directed against the Kv1.1 ectodomain, such that only 2.5 ± 1.2% of the Kv1.1-expressing cells exhibited detectable cell surface staining (Table I). By contrast, Kv1.4 was efficiently expressed on the surface, as evidenced by a lack of pronounced intracellular accumulation and a staining pattern consistent with plasma membrane localization. Moreover, 87.9 ± 4.6% of the cells expressing Kv1.4 exhibited robust staining (Fig. 1 E) with an externally directed antibody when staining was performed in the absence of detergent (Table I). Kv1.2 was intermediate between Kv1.1 and Kv1.4 in its surface expression (Ta-

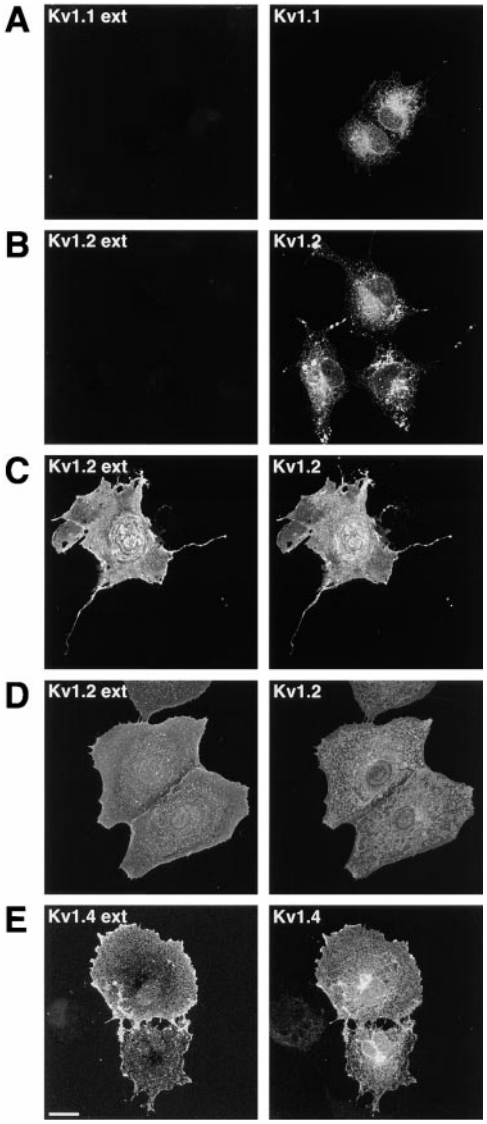

Figure 1. Immunofluorescence confocal microscopy analysis of the differential surface expression efficiency of the Kv1.1, Kv1.2, and Kv1.4 α subunits in transfected COS-1 cells. Each image represents a three-dimensional projection of the entire cell. (Left) External anti–Kv1 antibody staining performed in the absence of detergent permeabilization. (Right) cytoplasmic anti–Kv1 antibody staining performed after detergent permeabilization. (A) Kv1.1; (B and C) Kv1.2; (D) Kv1.2 + Kvβ2; and (E) Kv1.4. Bar, 20 μm.

Table I. Analysis of Kv Channel and MAGUK Expression in COS-1 Cells

Efficiency*	Kv1.1	Kv1.2	Kv1.2 + Kvβ2	Kv1.4
Surface expression	2.5 ± 1.1	23.3 ± 8.5	56.3 ± 4.2	87.9 ± 4.6
PSD-95 clustering	5.1 ± 1.0	18.5 ± 5.3	42.9 ± 12.4	72.4 ± 5.3
SAP97 clustering	50.7 ± 9.6	55.1 ± 7.3	53.9 ± 5.9	79.9 ± 7.9
Surface expression with PSD-95	3.4 ± 1.4	22.1 ± 3.3	49.4 ± 5.5	83.3 ± 1.4
Surface expression with SAP97	2.4 ± 1.0	13.0 ± 3.4	32.7 ± 6.9	22.0 ± 4.3

*Expressed as a percentage of total transfected cells expressing Kv α subunit that exhibit the respective staining. All values are mean ± SD of three independent samples of 50 transfected cells each.

ble I), with 23.3 ± 8.5% of the Kv1.2-expressing cells exhibiting surface staining (Fig. 1, B and C). This was true both on a per cell basis, in that intracellular and surface pools were present in the same cells, and on a population basis, with different cells exhibiting different proportions of the intracellular and surface pools (Fig. 1, compare B and C). In each case, the inherent surface expression properties of these Kv1 α subunits was independent of expression level and was reproduced in multiple cell lines of diverse origin (Manganas, L.N., and J.S. Trimmer, manuscript in preparation).

We previously found that coexpression of cytoplasmic β-subunits, which exhibit extensive association and colocalization with Kv1.2 α subunits in the mammalian brain (Rhodes et al., 1995, 1997) and in transfected COS cells (Nakahira et al., 1996), promote the surface expression of Kv1.2 (Shi et al., 1996). Consistent with these and other (Accili et al., 1997, 1998) previous studies, coexpression of Kvβ2 led to an increase in the percentage (56.3 ± 4.2%) of Kv1.2-expressing cells exhibiting surface staining (Fig. 1 D) relative to those expressing Kv1.2 alone (Table I).

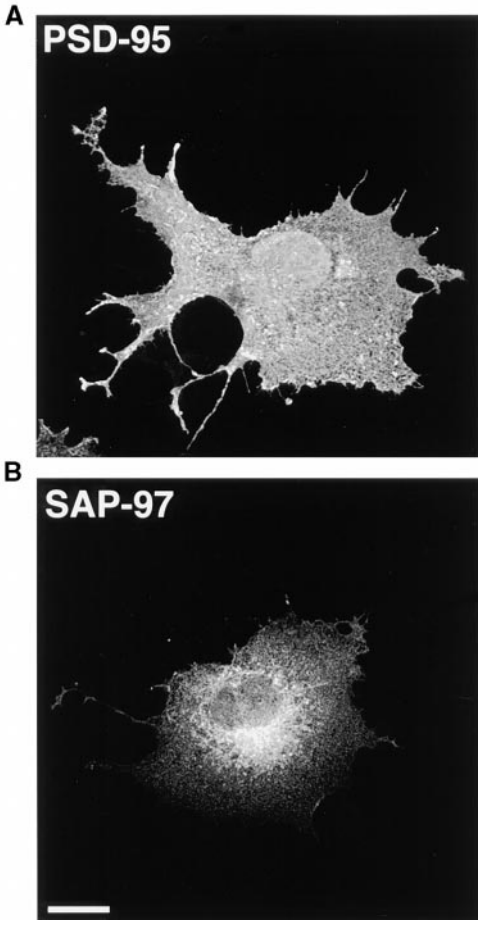

Figure 2. Immunofluorescence confocal microscopy analysis of the differential subcellular distribution of PSD-95 and SAP97 in transfected COS-1 cells. Each image represents a three-dimensional projection of the entire cell. (A) PSD-95; and (B) SAP97. Bar, 20 μm.

Highly Related MAGUKs Expressed in the Same Cell Background Have Different Subcellular Distributions

PSD-95 and SAP97 exhibit a high degree of sequence identity (73.6% amino acid identity) and the same overall domain structure, with three NH_2-terminal PDZ domains, a single SH3 domain, and a COOH-terminal guanylate kinase domain (Hata et al., 1998). However, when expressed in transfected COS-1 cells, these two polypeptides exhibit strikingly different subcellular distributions. PSD-95 is found mainly at the cell periphery (Fig. 2), presumably via an association with the plasma membrane mediated by palmitoylation (Topinka and Bredt, 1998; Craven et al., 1999). In contrast, SAP97 is present in perinuclear zones (Fig. 2), in a pattern resembling the ER.

Kv1 Clustering by PSD-95 Parallels Channel Cell Surface Expression Efficiency

The initial observation that MAGUKs cluster membrane proteins came from studies of PSD-95 and Kv1.4 (Kim et al., 1995). Subsequent studies showed that Kv1.4/PSD-95 clustering was quite efficient, although clustering of other Kv1 α subunits was not (Kim and Sheng, 1996). We found that the vast majority (Table I, 72.3 ± 5.3%) of cells coexpressing Kv1.4 and PSD-95 had these two proteins colocalized in plaquelike clusters similar to those observed in these previous studies (Fig. 3 D). The subcellular distributions of Kv1.4 and PSD-95 seen in cotransfected cells (Fig. 3 D) were dramatically different from those seen for either protein in singly transfected cells (Figs. 1 E and 2 A). However, coexpression of PSD-95 with the Kv1.1 α subunit, which exhibited a low level of cell surface expression (Table I), yielded a correspondingly low level of cells exhibiting clustering by PSD-95 (5.1 ± 1.0%). In cells coexpressing Kv1.1 and PSD-95 (Fig. 3 A), the subcellular distribution of the respective proteins seen in singly transfected cells remained unaltered by the presence of the other protein, suggesting not only a lack of clustering, but also a lack of interaction. Kv1.2 clustering by PSD-95 was intermediate in its efficiency (Table I), in that some cells (18.5 ± 5.3%) had clustered and colocalized Kv1.2 and PSD-95, resembling cells expressing Kv1.4 and PSD-95 (not shown), while the remainder of the population exhibited distinct and nonoverlapping subcellular distributions

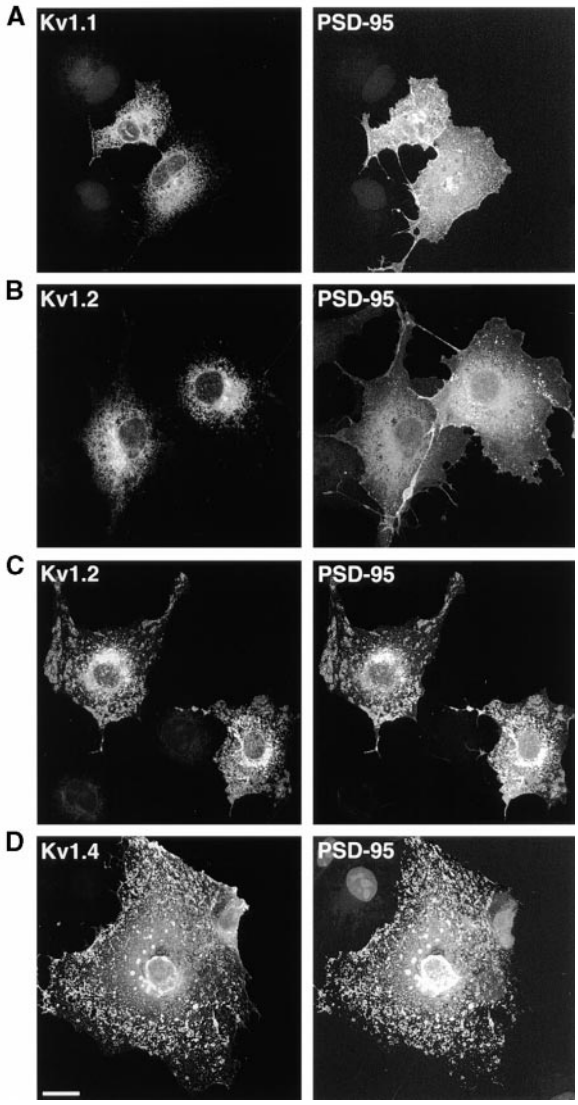

Figure 3. Clustering of Kv channels by coexpression with PSD-95. Immunofluorescence confocal microscopy was performed on cells coexpressing the Kv1 α subunits and PSD-95 and stained after detergent permeabilization. Each image represents a three-dimensional projection of the entire cell. (Left) Anti–Kv1 antibodies. (Right) Anti–MAGUK mAb K28/86. (A) Kv1.1; (B) Kv1.2; (C) Kv1.2 + Kvβ2; and (D) Kv1.4. Bar, 20 μm.

of the two proteins (Fig. 3 B), in a manner similar to that seen for cells expressing Kv1.1 and PSD-95. Overall, for all three of the Kv1 α subunits, the percentage of cells with PSD-95–induced clustering was similar to the percentage with cell surface expression (Table I). These results suggest that, for Kv1 α subunits, interaction with PSD-95 may depend on successful cell surface expression.

The three Kv1 α subunits examined exhibit small differences in the COOH-terminal PDZ binding motif, and exhibited different levels of binding to PSD-95 in the yeast two-hybrid system (Kim et al., 1995). Thus, the observed differences in the efficiency of clustering of Kv1 channels by PSD-95 could be due to these differences in binding efficiency, as suggested previously (Kim and Sheng, 1996). To address this question, we compared the PSD-95 clustering efficiency of the same α subunit, Kv1.2, in the presence and absence of β subunits. In this way, we could directly determine how PSD-95 clustering was affected by modulating surface expression efficiency in the absence of any differences in the COOH-terminal PDZ-binding motif. In cells coexpressing Kv1.2, Kvβ2, and PSD-95, Kv1.2 and PSD-95 were found coclustered (Fig. 3 C) in a much higher percentage of cells (42.9 ± 12.4%, $n = 3$) than in cells expressing Kv1.2 alone (Table I, 18.5 ± 5.3, $n = 3$). The effects of Kvβ2 on promoting the coclustering of Kv1.2 and PSD-95 occurred in a dose-dependent manner that paralleled the Kvβ2 effects on Kv1.2 surface expression (Table III). Coexpression of other Kvβ subunits, such as Kvβ1.1 and Kvβ1.2, also resulted in the more efficient surface expression of Kv1.2, and in more efficient coclustering of Kv1.2 and PSD-95 (not shown). Together these results suggest that the variability in the clustering of Kv1 channels by PSD-95 is primarily due to the differences in the surface expression efficiencies, and not the PSD-95 binding affinity, of the Kv1 α subunits.

SAP97 Differs from PSD-95 in Its Interaction with K^+ Channels

Kv1 channel/SAP97 coexpression yielded dramatically different results from those obtained with PSD-95. Coexpression resulted in the appearance of large perinuclear vesicles whose appearance was distinct from anything seen for Kv1–PSD-95 interaction (Fig. 4, A–D). Each of the Kv1 α subunits and SAP97 were extensively colocalized in these very large (3–5 μm diam) perinuclear structures (Fig. 4. A–D), which were not observed in cells expressing Kv1 channels or SAP97 alone (Figs. 1 and 2). These large vesicles were observed at many different ratios of SAP97:Kv1 α subunit expression. The only apparent effect of altering the relative expression levels of the Kv1 α subunit and SAP97 is on the proportion of the overall pool of each protein present in the clusters, and not in the clusters themselves (not shown). The fact that no such clusters are observed in cells expressing SAP97 alone (Fig. 2 B) nor in cells expressing SAP97 and a Kv1.4 mutant, which has an altered PDZ binding motif (ETDV changed to ETDA) and which does interact with SAP97, suggests that SAP97–Kv1 channel interaction in itself leads to the formation of these intracellular clusters.

Unlike the case with PSD-95, the efficiency of the interaction between SAP97 and the Kv1 α subunits did not correlate with channel surface expression efficiency (Table I). This is most obvious for Kv1.1, Kv1.2, and Kv1.2 + Kvβ2, which exhibit dramatically different cell surface expression efficiencies (∼2, ∼20, and ∼50%, respectively) but similar SAP97 clustering (∼50%, Table I). In fact, the pattern of SAP97 channel clustering efficiency (Kv1.4 > Kv1.1 ∼ Kv1.2 + Kvβ2 ∼ Kv1.2 alone) was quite similar to that seen for Kv1 α subunit: SAP97 binding in the yeast two-hybrid system (Kim et al., 1995). These results show that, in spite of the virtually identical interaction of these two highly related MAGUKs with Kv1 α subunits in the yeast two-hybrid system, PSD-95 and SAP97 differ substantially in their channel clustering mechanisms in mammalian cells.

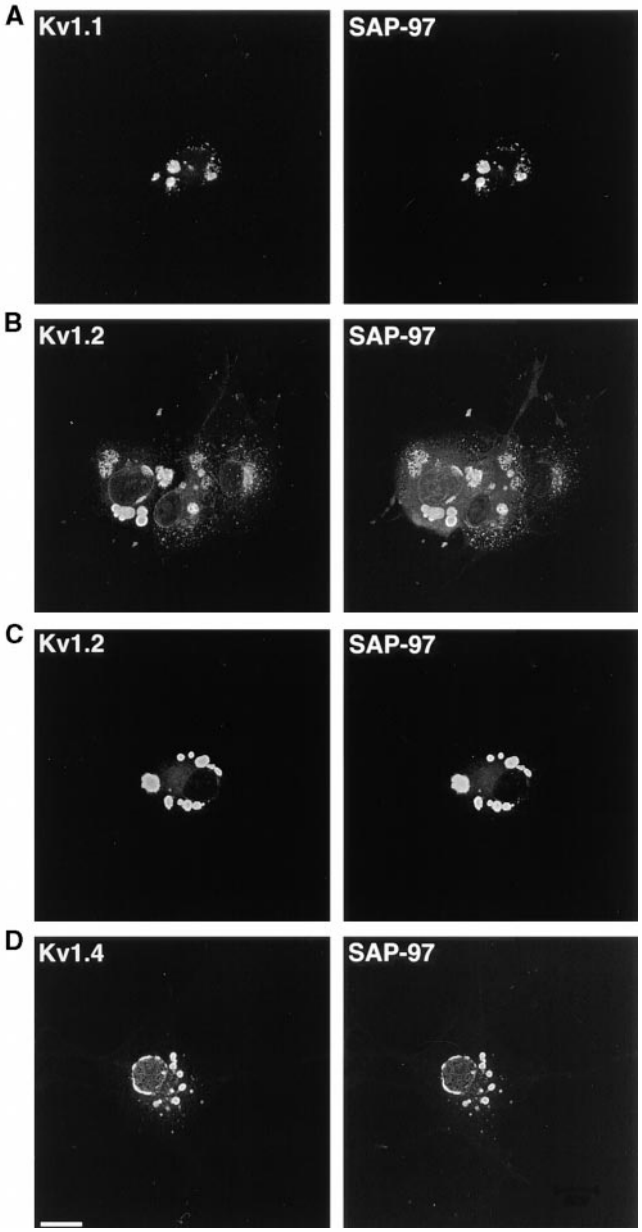

Figure 4. Clustering of Kv channels by coexpression with SAP97. Immunofluorescence confocal microscopy was performed on cells coexpressing the Kv1 α subunits and SAP97 and stained after detergent permeabilization. (Left) Cytoplasmic anti–Kv1 antibodies. (Right) Anti–MAGUK mAb K28/86. (A) Kv1.1; (B) Kv1.2; (C) Kv1.2 + Kvβ2; and (D) Kv1.4. Bar, 20 μm.

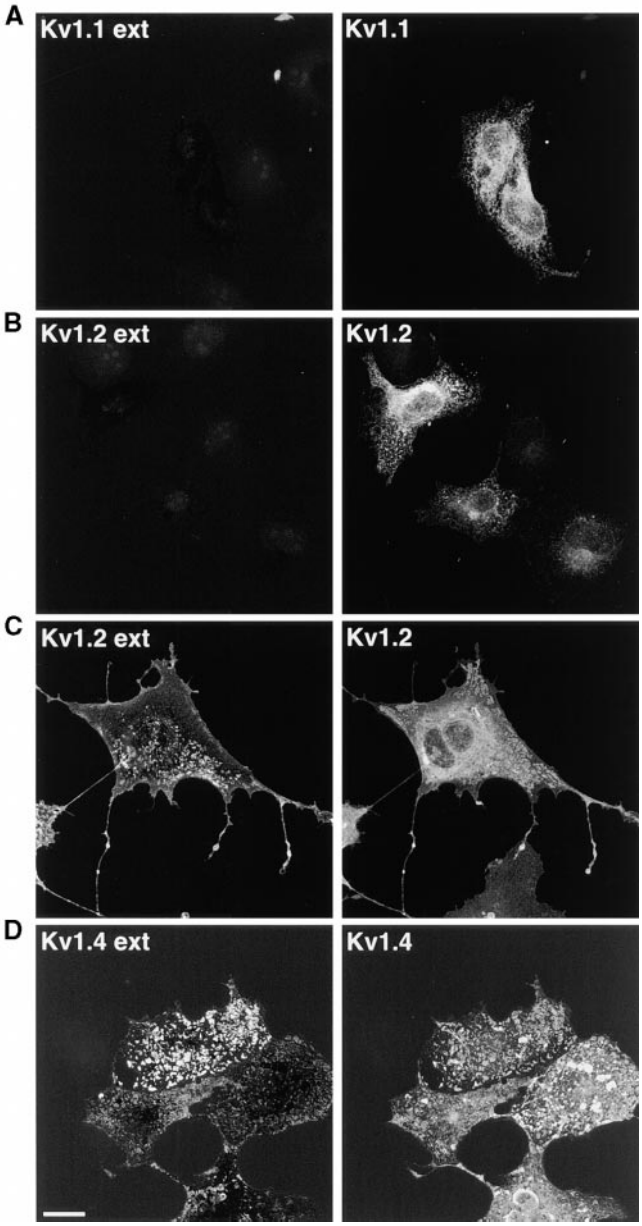

Figure 5. Immunofluorescence confocal microscopy analysis of the surface expression of the Kv1.1, Kv1.2, and Kv1.4 α subunits coexpressed with PSD-95 reveals the presence of cell surface clusters. (Left) External anti–Kv1 antibody staining performed in the absence of detergent permeabilization. Each image represents a three-dimensional projection of the entire cell. (Right) Cytoplasmic anti–Kv1 antibody staining performed after detergent permeabilization. (A) Kv1.1; (B) Kv1.2; (C) Kv1.2 + Kvβ2; and (D) Kv1.4. Bar, 20 μm.

Channels Clustered by PSD-95 Are Expressed on the Cell Surface

Since the initial report of K^+ channel clustering by PSD-95 (Kim et al., 1995), an important question has remained as to whether the clusters of K^+ channels induced by PSD-95 coexpression were, in fact, on the cell surface. In the case of clusters formed by PSD-95 interaction, clear surface staining of clustered Kv1.2 and Kv1.4 was observed (Fig. 5). Virtually all of the cells exhibiting PSD-95–mediated clustering of Kv1.2 and Kv1.4 had detectable cell surface clusters as detected by external antibody staining (not shown). However, the proportion of clusters that exhibited surface staining varied dramatically from cell to cell. Confocal microscopy revealed that a large fraction of the clusters that did not stain with external antibodies were found at the bottom of the cell, where cell–substratum interaction might interfere with external antibody access. Thus, the clusters on these adherent COS-1 cells that stain with externally applied antibodies may be an underestimate of the total surface clusters as they may reflect only

apical pools of channels. Consistent with this model, partial EDTA-mediated dissociation of cells from the substratum resulted in more extensive surface staining (not shown), presumably because of the increased antibody access to basal clusters. However, it is clear from these data that clusters formed by interaction of PSD-95 and Kv1 channels can exist on the cell surface.

PSD-95 coexpression has been shown to upregulate the expression of inward rectifier K^+ channels (Horio et al., 1997), suggesting that the channel-clustering MAGUKs could play an additional role in regulating channel abundance. Therefore, we tested whether PSD-95 influenced the cell surface expression efficiency of Kv1 channels. For all Kv1 subunits tested, coexpression of PSD-95 had little or no effect on channel surface expression efficiency (Table I). These results further suggest an interaction between Kv1 channels and PSD-95 at the level of the plasma membrane.

Inhibition of Kv1 Channel Surface Expression by SAP97

As discussed above, in cells coexpressing Kv1 channels and SAP97 both polypeptides were found in large, vesicular perinuclear clusters. Staining intact cells with ectodomain-directed antibodies revealed that in all cases these vesicular structures were intracellular (Fig. 6). Coexpression of these Kv1 α subunits with SAP97 also resulted in a dramatic decrease in surface channels (Table I). In fact, in each case, the magnitude of decrease in cell surface expression efficiency closely reflected the efficiency of SAP97 clustering, suggesting that the interaction with SAP97 led to the intracellular retention of the channels (Table II).

Because SAP97 clustering of Kv1 channels prevented surface expression, we next determined if the resultant intracellular vesicular clusters of channels represented a distinct biosynthetic step in the secretory pathway. First, untransfected cells were stained with antibodies against the resident ER protein BiP (Bole et al., 1986), or with *Lens culinaris* lectin (LCA), a marker for the COS cells Golgi apparatus (Hsu et al., 1992). As shown in Fig. 7 A, and as has been shown previously by others (Machamer et al., 1990), anti–BiP antibody labels a perinuclear compartment in COS-1 cells. In contrast, LCA staining was concentrated in a small patch, which was surrounded by the BiP staining (Fig. 7 A). Upon SAP97 and Kv1.4 coexpression, which resulted in the formation of typical large intracellular membranous structures, the BiP staining was dramatically altered (Fig. 7 B). The normal reticular pattern of BiP staining, representing ER morphology, was replaced by a pattern which colocalized with Kv1.4 in the large intracellular vesicles. In contrast, LCA staining was unaffected by SAP97/Kv1.4 coexpression, and remained in the tight patch as seen in untransfected cells (Fig. 7 C). The BiP-positive clusters of Kv1.4 and SAP97 were LCA-negative (Fig. 7 C), suggesting that the Kv1.4 and SAP97-containing large vesicular structures are derived from the ER, and not from the Golgi apparatus.

Biochemical analysis of Kv1.4 protein in cells expressing

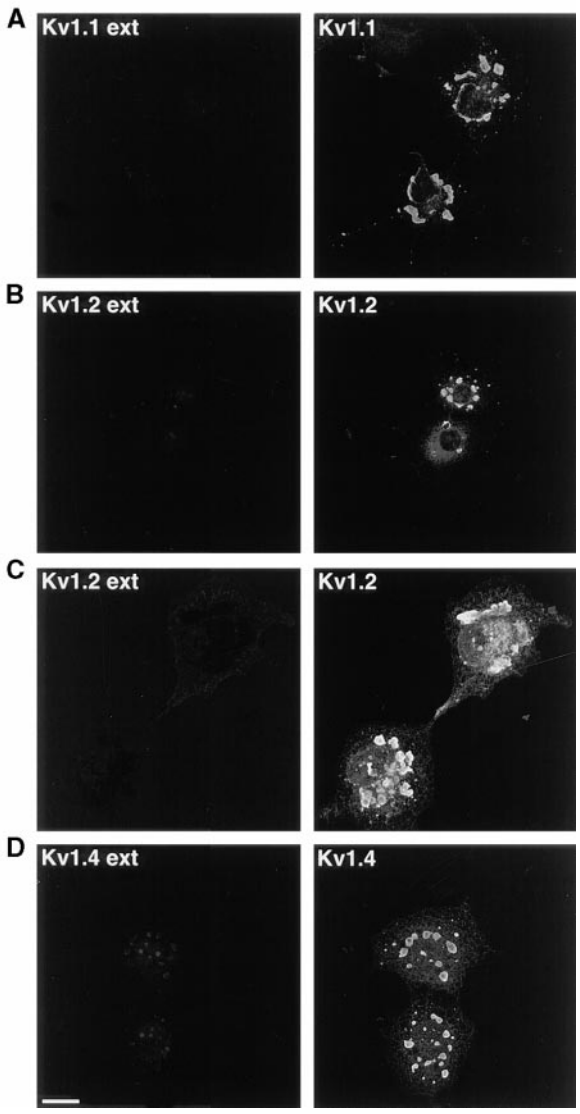

Figure 6. Immunofluorescence confocal microscopy analysis of the surface expression of the Kv1.1, Kv1.2, and Kv1.4 α subunits coexpressed with SAP97 reveals intracellular clusters. Each image represents a three-dimensional projection of the entire cell. (Left) External anti–Kv1 antibody staining performed in the absence of detergent permeabilization. (Right) Cytoplasmic anti–Kv1 antibody staining performed after detergent permeabilization. (A) Kv1.1; (B) Kv1.2; (C) Kv1.2 + Kvβ2; and (D) Kv1.4. Bar, 20 μm.

Table II. Kv1 K^+ Channel Surface Expression Efficiency with SAP97

Subunit	Theoretical*	Actual‡
Kv1.1	1.2	2.3 ± 1.0
Kv1.2	10.5	13.0 ± 3.4
Kv1.2 + Kvβ2	25.9	32.7 ± 6.9
Kv1.4	17.7	22.0 ± 4.3

*Calculated from the relationship: Theoretical Kv1 surface expression efficiency with SAP97 = (Kv1 inherent surface expression efficiency) (1-SAP97 clustering efficiency).
‡Values from Table I. Note that all theoretical values are within 1 SD unit of actual values.

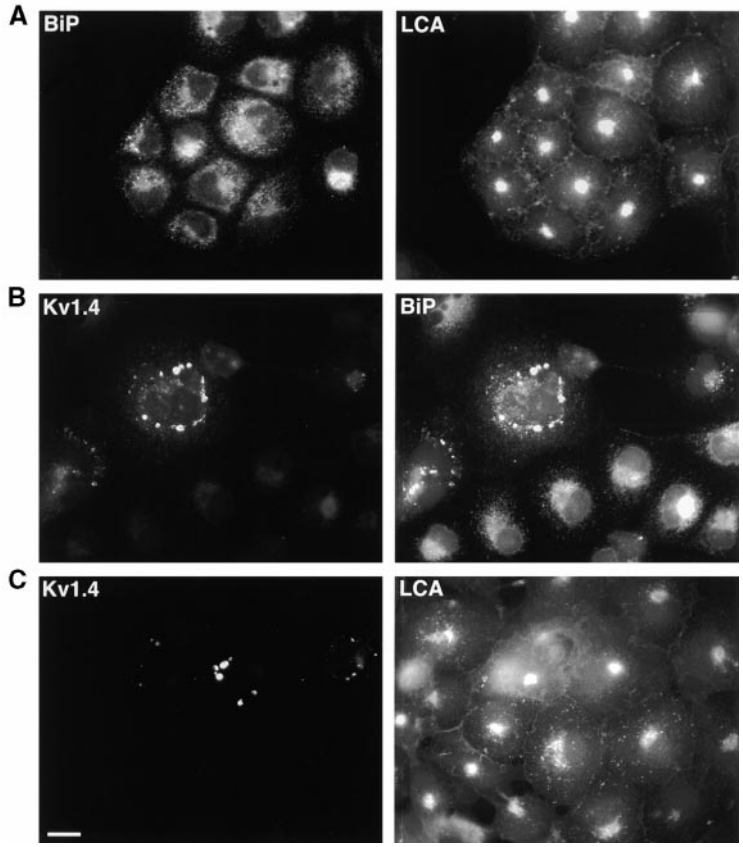

Figure 7. Intracellular complexes of Kv1.4 and SAP97 are derived from the ER. Immunofluorescence analysis of Kv1.4 α subunits coexpressed with SAP97 reveals intracellular clusters that colocalize with staining obtained with a monoclonal anti–BiP antibody, but not with the Golgi marker LCA lectin. (A) Untransfected cells; and (B and C) cells coexpressing Kv1.4 + SAP97.

PSD-95 and SAP97 supported the conclusion that association with SAP97 retains Kv1.4 in an ER-derived compartment. Kv1.4 contains a single N-linked oligosaccharide chain attached to Asn^{207} in the extracellular segment between the S1 and S2 transmembrane domains. In COS cells expressing Kv1.4 alone, Kv1.4 is processed from an 86-kD precursor form containing a high mannose oligosaccharide chain to a mature 110-kD form with a complex, sialidated N-glycan (Shi and Trimmer, 1999). Under steady state conditions, this results in a predominance of processed Kv1.4 in cells expressing Kv1.4 alone 48 h after transfection (Fig. 8). The mean densitometric ratio of the upper to lower band intensity in samples prepared from these cells was 1.24 (± 0.01, $n = 4$). In cells coexpressing Kv1.4 and PSD-95, a similar pattern was observed (Fig. 8), with only a slight decrease in the ratio of processed to unprocessed Kv1.4 (0.98 ± 0.02, $n = 4$). However, coexpression with SAP97 yields a dramatically different pattern (Fig. 8). The intensity of the upper molecular weight band was significantly reduced (Fig. 8), so that the ratio of the upper to lower Kv1.4 band was reduced to 0.08 (± 0.03, $n = 4$). These data, together with the immunostaining results, provide compelling evidence that Kv1.4–SAP97 interaction inhibits Kv1.4 transit through the endomembrane system at the level of the ER, resulting in the formation of large ER-derived intracellular vesicles.

Targeting of PSD-95 and SAP97 in Transfected Cells

We have generated an SAP97 mutant (ΔN-SAP97) lacking the first 108 amino acids of the unique SAP97 NH_2-terminal domain. When expressed in transfected cells, this SAP97 mutant (Fig. 9 B) like wild-type SAP97 (Fig. 9 A) is associated with the ER, showing that the bulk of the unique NH_2 terminus of SAP97 is not necessary for ER targeting. When coexpressed with Kv1.1, the DN-SAP97 mutant exhibits precise colocalization with Kv1.1 in the ER (Fig. 9 D). Interestingly, the large intracellular clusters seen upon wild-type SAP97/Kv1.1 coexpression (Fig. 9 C, also see Fig. 4 A) are not apparent. We conclude from these results that the deleted 108–amino acid portion of the unique SAP97 NH_2 terminus does not contain the SAP97

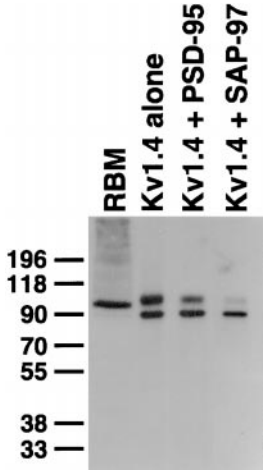

Figure 8. Immunoblot analysis shows different forms of Kv1.4 in cells expressing Kv1.4 alone, or coexpressing PSD-95 or SAP97. Enhanced chemiluminescence exposure times: RBM, Kv1.4 alone and Kv1.4 + PSD-95 lanes: 7 min, Kv1.4 + SAP97 lane: 25 min.

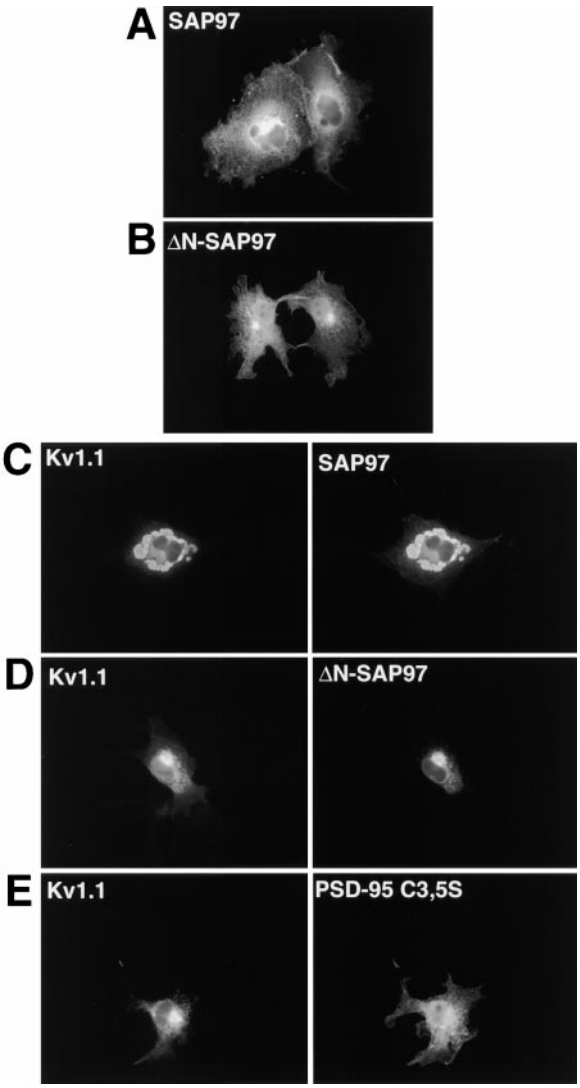

Figure 9. Distributions of SAP97 and PSD-95 deletion mutants. Immunofluorescence analysis of cells expressing MAGUKs alone (A and B) or coexpressing the Kv1.1 α subunit and MAGUKs (C–E) and stained after detergent permeabilization. (A and B and right panels of C–E) Anti–MAGUK mAb K28/8. Left panels of C–E: cytoplasmic anti-Kv1.1 polyclonal antibody. (A) Wild-type SAP97; (B) ΔN-SAP97 mutant; (C) Kv1.1 + wild-type SAP97; (D) Kv1.1 + ΔN-SAP97 mutant; and (E) Kv1.1 + PSD-95 C3,5S mutant.

ER targeting signal, although it apparently contains a domain necessary for SAP97–Kv1 channel clustering.

We next turned to PSD-95 targeting to the plasma membrane. Cysteines at positions 3 and 5 of PSD-95 are post-translationally modified with palmitate, whereas SAP97 lacks analogous cysteine residues and, thus, is not palmitoylated (Topinka and Bredt, 1998). Mutating these residues and preventing palmitoylation disrupts PSD-95 association with membranes (Topinka and Bredt, 1998). We have mutated these same cysteines and found no effects on Kv1.4 interaction, but did observe a loss of Kv1.4 clustering due to disruption of PSD-95 multimerization (Hsueh et al., 1997; Hsueh and Sheng, 1999). We also observed a lack of plasma membrane localization for this mutant (not shown). Interestingly, this mutant does not localize to the ER, or interact with coexpressed Kv1.1 (Fig. 9 E). These results together show that simply removing palmitoylation of PSD-95 does not result in a SAP97-like phenotype, and reinforces the notion that SAP97 contains specific sequences that target this MAGUK to ER and allow it to interact with ER-localized Kv1 channels.

Table III. Kvβ2 Effects on Kv1.2 Surface Expression and Clustering by PSD-95

β/α-subunit ratio	Surface expression*	Clustering*
0	22.5 ± 2.1	34.0 ± 2.0
1	35.5 ± 3.5	36.0 ± 1.4
2	38.0 ± 0.1	48.0 ± 6.9
4	41.5 ± 6.4	60.0 ± 4.0
8	26.0 ± 2.0	42.0 ± 2.0

*Expressed as a percentage of total transfected cells expressing Kv α subunit that exhibit the respective staining. All values are mean ± SD of three independent samples of 50 transfected cells each.

Discussion

Subcellular Distributions of Kv Channels and MAGUKs

Although Kv1.1, Kv1.2, and Kv1.4 are highly related at the amino acid level (Kv1.1/Kv1.2 = 80.3%; Kv1.2/Kv1.4 = 67.7%; Kv1.1/Kv1.4 = 70.0%), they differ dramatically in their intracellular trafficking and cell surface expression when expressed as homotetramers in transfected cells. The majority of Kv1.1 and Kv1.2 remain inside cells, presumably within the ER, as the N-linked oligosaccharide chains remain in an endoglycosidase H–sensitive high mannose form (Shi and Trimmer, 1999). In contrast, Kv1.4 is expressed on the cell surface, and exhibits efficient Golgi-based processing of its N-linked glycan (Shi and Trimmer, 1999). The mechanisms underlying these differences are unknown, as are the determinants within the channel polypeptides.

PSD-95 and SAP97, members of a large and highly related gene family, exhibit 73.6% amino acid identity, and have the same basic domain structure. However, as shown here, in transfected COS-1 cells, PSD-95 and SAP97 have distinct subcellular distributions. In neurons, PSD-95 is found in the somatodendritic domain and is preferentially localized to postsynaptic sites where it is a major component of the postsynaptic density (Kennedy, 1997). In transfected COS-1 cells, PSD-95 is found at the cell periphery in the cytoskeleton-rich cell cortex, and immobilizes target proteins such as Kv1.4 at the plasma membrane of transfected cells (Burke et al., 1999), presumably through an interaction with the cytoskeleton (Niethammer et al., 1998). Interaction with cell adhesion molecules may also contribute to the immobilization of PSD-95 at the plasma membrane (Irie et al., 1997). PSD-95 has also been found to be covalently modified with the fatty acid palmitate on cysteine residues located near the NH_2 terminus (Topinka and Bredt, 1998). In contrast, SAP97 has an extended (160 amino acid) NH_2 terminus that lacks the palmitoylation sites present on PSD-95. Palmitoylation of PSD-95 results in its preferential association with membranes and, in neu-

rons, targeting to synapses; neither unpalmitoylated PSD-95 mutants nor wild-type SAP97 exhibit these characteristics (Craven et al., 1999). The NH_2-terminal cysteines of PSD-95 also play a role in the multimerization of PSD-95 that is required for simultaneous binding of multiple membrane protein ligands and clustering of PSD-95 and target proteins (Hsueh et al., 1997; Hsueh and Sheng, 1999). Here, we found that a mutation of these same cysteines do not convert PSD-95 into a SAP97-like phenotype, as we do not observe SAP97-like ER-targeting or interaction with ER-localized Kv1 α subunits in the PSD-95 double cysteine mutant.

In neurons, SAP97 is reported to be axonal and presynaptic, suggesting efficient transport from the somatodendritic domain, which contains the bulk of the neuron's biosynthetic machinery, to the axon with little accumulation at the site of synthesis (Muller et al., 1995). In epithelial CACO-2 cells, SAP97 is associated with the cortical actin cytoskeleton at sites of cell–cell adhesion in the lateral membranes, again with little apparent intracellular accumulation (Reuver and Garner, 1998; Wu et al., 1998). The first 65 amino acids of the unique SAP97 NH_2-terminal domain are necessary for this association with cell–cell contact zones (Wu et al., 1998). In transfected COS-1 cells, SAP97 is predominantly perinuclear. The association with ER is surprising for a protein synthesized from free cytoplasmic ribosomes and may indicate that SAP97 contains a domain that associates with a component of the ER. We found that deleting the first 108 amino acids of the unique SAP97 NH_2 terminus did not affect ER targeting, or the ability of SAP97 to interact with ER-localized channels. Thus, targeting of SAP97 in COS-1 cells differs from that observed in CACO-2 cells in both the ultimate subcellular localization and in the targeting determinant itself. However, deletion of these 108 NH_2-terminal amino acids of SAP97 did eliminate the formation of the large intracellular clusters upon interaction with Kv1.1. These data suggest a role for the NH_2 terminus in mediating the heteromultimerization of SAP97 and Kv1 channels that leads to clustering. A similar role has been shown for the unrelated NH_2 terminus of PSD-95 (Hsueh et al., 1997; Hsueh and Sheng, 1999). Future studies will reveal the precise ER targeting signal on SAP97 and its role in MAGUK-mediated regulation of ion channel trafficking and surface expression.

PSD-95 Clustering Efficiency Is Dependent on Kv1 Surface Expression and Not on PDZ Domain Binding Affinity

All Kv1 α subunits display specific binding to PSD-95 and SAP97 in cell-free systems, and when COOH-terminal fragments are used as interaction bait in the yeast two-hybrid system (Kim et al., 1995). However, as shown originally by Kim and Sheng (1996), the clustering efficiency by PSD-95 in their cotransfection assay differs considerably for different subunits. The authors attributed this to differences to the relative binding affinity of the channels for PSD-95 because of small differences in the COOH-terminal PDZ binding motif (Kim and Sheng, 1996). However, we find that a stronger correlation exists between channel surface expression and PSD-95 clustering. This suggests that surface expression is required for PSD-95 clustering, and that a more likely explanation for differences in clustering are the inherent differences in Kv1 channel cell surface expression. The data on Kv1.2 clustering in the presence and absence of cytoplasmic β subunits provide the most compelling evidence for this model. The binding affinity of Kv1.2 for PSD-95 should remain unaffected by β subunit coexpression, since the COOH terminus of Kv1.2, which contains the PDZ-binding motif, is present regardless of the β subunit expression level. However, dramatic increases in PSD-95 clustering of Kv1.2 were observed upon β subunit coexpression. Given that β subunit coexpression has similar effects on Kv1.2 cell surface expression efficiency (Shi et al., 1996), it seems likely that the increases in PSD-95 clustering upon β subunit coexpression occur indirectly through β subunit-mediated promotion of surface expression.

Effects of MAGUKs on Surface Expression

Previous studies showed that coexpression of either PSD-95 or SAP97 increased the density of Kir4.1 currents in transfected cells by increasing the number of functional channels (Horio et al., 1997). The authors proposed that PSD-95 and SAP97 may play an important biosynthetic role in facilitating the surface expression of Kir4.1. We have investigated the effects of these same MAGUKs on Kv1 channel expression. Using an approach we have used previously to examine the effects of cytoplasmic Kvβ subunits (Shi et al., 1996), we found that PSD-95 had no effect on the surface expression efficiency of Kv1 α subunits, either in the presence or absence of auxiliary β subunits. This lack of a pronounced biosynthetic effect is consistent with a model whereby PSD-95 and Kv1 channels initially encounter one another at or near the plasma membrane. Thus, PSD-95 may function to anchor Kv1 channels at designated plasma membrane sites rather than mediate their dynamic intracellular targeting. A recent study characterized the localization of recombinant PSD-95 and Kv1.4 expressed singly or together in organotypic cortical slice cultures and was consistent with a model where PSD-95 itself does not contain prominent subcellular targeting information (Arnold and Clapham, 1999).

Surprisingly, unlike its effects on Kir4.1, and distinct from the neutral role of PSD-95, SAP97 proved to be a potent inhibitor of Kv1 channel surface expression. We conclude that SAP97 interacts with newly synthesized Kv1 channels while the latter are still in the ER, preventing their subsequent export. In addition, the coexpression and interaction of SAP97 and Kv1 K^+ channels had dramatic effects on the morphology of the ER itself, causing this reticular network to fuse into several large intracellular membranous structures that contain all of the detectable immunoreactivity for both BiP, and for SAP97–Kv1 complexes. Perhaps in neurons, the efficient targeting of SAP97 to axons, away from the somal endomembrane components of the secretory pathway, prevents intracellular association of SAP97 and newly synthesized Kv1 channels. Alternatively, Kv1–SAP97 interaction in neurons could occur intracellularly, as in COS-1 cells, but neuronal-specific transport mechanisms cells could ensure the efficient targeting of the prepackaged complexes to axonal

sites. Future studies may elucidate the role that PSD-95, SAP97, and other MAGUKs play in determining the abundance and distribution of Kv1 channels as critical regulators of membrane excitability in neurons.

The authors thank Drs. Gail Mandel, Matthew N. Rasband (both from SUNY Stony Brook), and Kenneth J. Rhodes (Wyeth-Ayerst Research) for critically reviewing this manuscript, and to Ms. Joan Speh (SUNY Stony Brook) and Dr. Gail Mandel for the use of the confocal microscope.

This work was supported by the National Institutes of Health grant NS34383 to J.S. Trimmer.

Submitted: 31 August 1999
Revised: 23 November 1999
Accepted: 7 December 1999

References

Accili, E.A., J. Kiehn, Q. Yang, Z. Wang, A.M. Brown, and B.A. Wible. 1997. Separable Kvbeta subunit domains alter expression and gating of potassium channels. *J. Biol. Chem*. 272:25824–25831.

Accili, E.A., Y.A. Kuryshev, B.A. Wible, and A.M. Brown. 1998. Separable effects of human Kvbeta1.2 N- and C-termini on inactivation and expression of human Kv1.4. *J. Physiol*. 512:325–336.

Arnold, D.B., and D.E. Clapham. 1999. Molecular determinants for subcellular localization of PSD-95 with an interacting K^+ channel. *Neuron*. 23:149–157.

Bekele-Arcuri, Z., M.F. Matos, L. Manganas, B.W. Strassle, M.M. Monaghan, K.J. Rhodes, and J.S. Trimmer. 1996. Generation and characterization of subtype-specific monoclonal antibodies to K^+ channel alpha- and beta-subunit polypeptides. *Neuropharmacology*. 35:851–865.

Bole, D.G., L.M. Hendershot, and J.F. Kearney. 1986. Posttranslational association of immunoglobulin heavy chain binding protein with nascent heavy chains in nonsecreting and secreting hybridomas. *J. Cell Biol*. 102:1558–1566.

Burke, N.A., K. Takimoto, D. Li, W. Han, S.C. Watkins, and E.S. Levitan. 1999. Distinct structural requirements for clustering and immobilization of K^+ channels by PSD-95. *J. Gen. Physiol*. 113:71–80.

Chandy, K.G., and G.A. Gutman. 1995. Voltage-gated potassium channel genes. *In* Ligand- and Voltage-gated Ion Channels. R.A. North, editor. CRC Press, Boca Raton, FL. 1–71.

Cooper, E.C., A. Milroy, Y.N. Jan, L.Y. Jan, and D.H. Lowenstein. 1998. Presynaptic localization of Kv1.4-containing A-type potassium channels near excitatory synapses in the hippocampus. *J. Neurosci*. 18:965–974.

Craven, S.E., A.E. El-Husseini, and D.S. Bredt. 1999. Synaptic targeting of the postsynaptic density protein PSD-95 mediated by lipid and protein motifs. *Neuron*. 22:497–509.

Doyle, D.A., A. Lee, J. Lewis, E. Kim, M. Sheng, and R. MacKinnon. 1996. Crystal structures of a complexed and peptide-free membrane protein-binding domain: molecular basis of peptide recognition by PDZ. *Cell*. 85:1067–1076.

Hata, Y., H. Nakanishi, and Y. Takai. 1998. Synaptic PDZ domain-containing proteins. *Neurosci. Res*. 32:1–7.

Horio, Y., H. Hibino, A. Inanobe, M. Yamada, M. Ishii, Y. Tada, E. Satoh, Y. Hata, Y. Takai, and Y. Kurachi. 1997. Clustering and enhanced activity of an inwardly rectifying potassium channel, Kir4.1, by an anchoring protein, PSD-95/SAP90. *J. Biol. Chem*. 272:12885–12888.

Hsu, V.W., N. Shah, and R.D. Klausner. 1992. A brefeldin A-like phenotype is induced by the overexpression of a human ERD-2-like protein, ELP-1. *Cell*. 69:625–635.

Hsueh, Y.P., E. Kim, and M. Sheng. 1997. Disulfide-linked head-to-head multimerization in the mechanism of ion channel clustering by PSD-95. *Neuron*. 18:803–814.

Hsueh, Y.P., and M. Sheng. 1999. Requirement of N-terminal cysteines of PSD-95 for PSD-95 multimerization and ternary complex formation, but not for binding to potassium channel Kv1.4. *J. Biol. Chem*. 274:532–536.

Irie, M., Y. Hata, M. Takeuchi, K. Ichtchenko, A. Toyoda, K. Hirao, Y. Takai, T.W. Rosahl, and T.C. Sudhof. 1997. Binding of neuroligins to PSD-95. *Science*. 277:1511–1515.

Kennedy, M.B. 1997. The postsynaptic density at glutamatergic synapses. *Trends Neurosci*. 20:264–268.

Kim, E., and M. Sheng. 1996. Differential K^+ channel clustering activity of PSD-95 and SAP97, two related membrane-associated putative guanylate kinases. *Neuropharmacology*. 35:993–1000.

Kim, E., M. Niethammer, A. Rothschild, Y.N. Jan, and M. Sheng. 1995. Clustering of Shaker-type K^+ channels by interaction with a family of membrane-associated guanylate kinases. *Nature*. 378:85–88.

Laube, G., J. Roper, J.C. Pitt, S. Sewing, U. Kistner, C.C. Garner, O. Pongs, and R.W. Veh. 1996. Ultrastructural localization of Shaker-related potassium channel subunits and synapse-associated protein 90 to septate-like junctions in rat cerebellar Pinceaux. *Brain Res. Mol. Brain Res*. 42:51–61.

Machamer, C.E., R.W. Doms, D.G. Bole, A. Helenius, and J.K. Rose. 1990. Heavy chain binding protein recognizes incompletely disulfide-bonded forms of vesicular stomatitis virus G protein. *J. Biol. Chem*. 265:6879–6883.

Muller, B.M., U. Kistner, R.W. Veh, C. Cases-Langhoff, B. Becker, E.D. Gundelfinger, and C.C. Garner. 1995. Molecular characterization and spatial distribution of SAP97, a novel presynaptic protein homologous to SAP90 and the *Drosophila* discs-large tumor suppressor protein. *J. Neurosci*. 15:2354–2366.

Nakahira, K., G. Shi, K.J. Rhodes, and J.S. Trimmer. 1996. Selective interaction of voltage-gated K^+ channel beta-subunits with alpha-subunits. *J. Biol. Chem*. 271:7084–7089.

Niethammer, M., J.G. Valtschanoff, T.M. Kapoor, D.W. Allison, T.M. Weinberg, A.M. Craig, and M. Sheng. 1998. CRIPT, a novel postsynaptic protein that binds to the third PDZ domain of PSD-95/SAP90. *Neuron*. 20:693–707.

Rasband, M.N., J.S. Trimmer, T.L. Schwarz, S.R. Levinson, M.H. Ellisman, M. Schachner, and P. Shrager. 1998. Potassium channel distribution, clustering, and function in remyelinating rat axons. *J. Neurosci*. 18:36–47.

Reuver, S.M., and C.C. Garner. 1998. E-cadherin mediated cell adhesion recruits SAP97 into the cortical cytoskeleton. *J. Cell Sci*. 111:1071–1080.

Rhodes, K.J., S.A. Keilbaugh, N.X. Barrezueta, K.L. Lopez, and J.S. Trimmer. 1995. Association and colocalization of K^+ channel alpha- and beta-subunit polypeptides in rat brain. *J. Neurosci*. 15:5360–5371.

Rhodes, K.J., M.M. Monaghan, N.X. Barrezueta, S. Nawoschik, Z. Bekele-Arcuri, M.F. Matos, K. Nakahira, L.E. Schechter, and J.S. Trimmer. 1996. Voltage-gated K^+ channel beta subunits: expression and distribution of Kv beta 1 and Kv beta 2 in adult rat brain. *J. Neurosci*. 16:4846–4860.

Rhodes, K.J., B.W. Strassle, M.M. Monaghan, Z. Bekele-Arcuri, M.F. Matos, and J.S. Trimmer. 1997. Association and colocalization of the Kvbeta1 and Kvbeta2 beta-subunits with Kv1 alpha-subunits in mammalian brain K+ channel complexes. *J. Neurosci*. 17:8246–8258.

Scannevin, R.H., H. Murakoshi, K.J. Rhodes, and J.S. Trimmer. 1996. Identification of a cytoplasmic domain important in the polarized expression and clustering of the Kv2.1 K^+ channel. *J. Cell Biol*. 135:1619–1632.

Scannevin, R.H., and J.S. Trimmer. 1997. Cytoplasmic domains of voltage-sensitive K^+ channels involved in mediating protein-protein interactions. *Biochem. Biophys. Res. Comm*. 232:585–589.

Sheng, M., and M. Wyszynski. 1997. Ion channel targeting in neurons. *Bioessays*. 19:847–853.

Shi, G., and J.S. Trimmer. 1999. Differential asparagine-linked glycosylation of voltage-gated K^+ channels in mammalian brain and in transfected cells. *J. Membr. Biol*. 168:265–273.

Shi, G., A.K. Kleinklaus, N.V. Marrion, and J.S. Trimmer. 1994. Properties of Kv2.1 K^+ channels expressed in transfected mammalian cells. *J. Biol. Chem*. 269:23204–23211.

Shi, G., K. Nakahira, S. Hammond, K.J. Rhodes, L.E. Schechter, and J.S. Trimmer. 1996. Beta subunits promote K^+ channel surface expression through effects early in biosynthesis. *Neuron*. 16:843–852.

Shih, T.M., and A.L. Goldin. 1997. Topology of the Shaker potassium channel probed with hydrophilic epitope insertions. *J. Cell Biol*. 136:1037–1045.

Topinka, J.R., and D.S. Bredt. 1998. N-terminal palmitoylation of PSD-95 regulates association with cell membranes and interaction with K^+ channel Kv1.4. *Neuron*. 20:125–134.

Trimmer, J.S. 1998a. Analysis of K^+ channel biosynthesis and assembly in transfected mammalian cells. *Methods Enzymol*. 293:32–49.

Trimmer, J.S. 1998b. Regulation of ion channel expression by cytoplasmic subunits. *Curr. Opin. Neurobiol*. 8:370–374.

Trimmer, J.S. 1999. Sorting out receptor trafficking. *Neuron*. 22:411–412.

Trimmer, J.S., and K.J. Rhodes. 1999. Heteromultimer formation in native K^+ channels. *In* Potassium Channels in Cardiovascular Biology. S. Archer and N. Rusch, editors. Plenum Press, New York.

Trimmer, J.S., I.S. Trowbridge, and V.D. Vacquier. 1985. Monoclonal antibody to a membrane glycoprotein inhibits the acrosome reaction and associated Ca^{2+} and H^+ fluxes of sea urchin sperm. *Cell*. 40:697–703.

Wang, H., D.D. Kunkel, T.M. Martin, P.A. Schwartzkroin, and B.L. Tempel. 1993. Heteromultimeric K^+ channels in terminal and juxtaparanodal regions of neurons. *Nature*. 365:75–79.

Wu, H., S.M. Reuver, S. Kuhlendahl, W.J. Chung, and C.C. Garner. 1998. Subcellular targeting and cytoskeletal attachment of SAP97 to the epithelial lateral membrane. *J. Cell Sci*. 111:2365–2376.